Transactions of the Materials Research Society of Japan 30[4] 1031-1035 (2005)

Stabilization of Deposition Rate of Mn Oxide Films by using SUS Cell

Masaaki Isai*, Yutaka Nagashio, Tomohiro Tatei and Hiroshi Fujiyasu
Department of Electrical and Electronic Engineering, Shizuoka University, 3-5-1 Johoku , Hamamatsu, Shizuoka, Japan 432-8561
*Electronic mail: temisai@ipc.shizuoka.ac.jp

Manganese oxide films for lithium secondary batteries were prepared using a reactive evaporation method. The Mn metal suffers oxidation since it is evaporated in the oxygen atmosphere. So the deposition rate is deteriorated with increasing deposition run. This paper shows a technique which keeps off the Mn evaporant from oxygen atmosphere during the reactive evaporation process. A stainless steel cell (SUS cell) which has been installed in the bottom of the Mn crucible. The Mn_3O_4 films could be prepared with high reproducibility with this SUS cell. The effect of SUS cell length on the crystal properties was investigated.

KEYWORDS: manganese oxide films, lithium secondary batteries, reactive evaporation, vacuum deposition, hausmannite structure

1. Introduction

Revolution of energy sources for electric vehicles has been started by using fuel cells and Lithium (Li) secondary batteries. Its success depends on the high rate discharge properties of secondary batteries. These devices require energy density more than 100 Wh/kg and power density more than 40 W/kg.[1] The low energy storage applications have been widely spread for a cellular phone and a camcoder and so on. There are a lot of potential candidate materials for secondary batteries.[1,2] A combination of manganese (Mn) oxide and Li was considered as the positive and negative electrodes, respectively. An operating voltage of 3～4 V can be obtained by this system.

Structural characteristics and theoretical capacities of defect spinels have been investigated.[3,4] Defect spinel is defined by the Mn_3O_4 – $Li_4Mn_5O_{12}$–λ-MnO_2 triangle in the Li-Mn-O phase diagram. Stoichiometric spinel phase is also defined by the Mn_3O_4– $Li_4Mn_5O_{12}$ line. The λ-MnO_2 has the highest theoretical capacity of 308 mAh/g in the defect spinels. But, it has highly oxidizing character over the compositional range $0 \leqq x \leqq 1$ in $Li_x[Mn_2]O_4$. Mn_3O_4 has the theoretical capacity of 117 mAh/g. Our goal is to prepare defect spinels defined by the $LiMn_2O_4$ – $Li_2Mn_4O_9$ – $Li_4Mn_5O_{12}$ triangle. These defect spinels would have generally a high structural stability upon lithiation. The theoretical capacity of the materials in this triangle scatters between 148 and 213 mAh/g. These materials are appropriate for the batteries of electric vehicles.

Almost all the oxide powders for positive electrodes are prepared by the sintering.[3-13] These powders have to be mixed with some binders and high electric conductivity materials like carbon black to apply the metal electrode. This process has complex procedures and induces thick films. This is less attractive in the point of energy density than the deposition process proposed in this paper.

Mn oxide films have been prepared by using many deposition methods.[14-32] The Mn_3O_4 films with spinel structure have been successfully prepared using a reactive evaporation method in our early works. [26-31] They are so called Hausmannite. The Li-Mn-O phase diagrams[3,4] show that defect spinels could be prepared by reacting the Li atoms with Mn_3O_4 as well as with λ-MnO_2.[5,6]

The reactive evaporation brings oxidation of Mn metal in the crucible (Mn evaporant) from oxygen atmosphere. The deposition rate is decreased run by run because of growing the thickness of oxidation layer which covers the metallic Mn. The three methods which overcomes the oxidation of Mn evaporant have been invented, for example, a Mo (molybdenum) separator[26-30], a stainless steel (SUS) cell[31] and a quartz ampoule.[32] The effectiveness of SUS cell in these devices was shown in the previous paper.[31] The aim of this study is to evaluate the effect of SUS cell length on the oxidation of Mn evaporant. This SUS cell has a composition of 18 Cr-8 Ni and this is so called SUS304.

The purpose of the present work is to evaluate the ability of SUS cell by which the oxidation of Mn evaporant is successfully prevented during the evaporation process.

2. Experiment

Mn oxide films were prepared on aluminum substrates by Hotwall epitaxy. Deposition apparatus is shown in Fig. 1. Mn metal was evaporated in the oxygen atmosphere. The oxygen (O_2) flow rate was controlled by a mass flow controller. The O_2 flow rate was fixed at 5 standard cubic centimeter per minute (sccm). The wall (T_{wall}) temperature was fixed at 800℃ through this study. The stainless steel crucible was heated by an electric resistance wire.

A SUS cell with a small hole was set in the bottom of the crucible, which contained Mn evaporant. The hole diameter was 6 mm. It acts as a separator which keeps Mn evaporant off the oxygen atoms. The length of SUS cell was varied from 10 to 70 mm. The source (T_{source}) temperature of the crucible was varied from 815, 835 and 870℃ for the length of SUS cell of 10, 30 and 50, 70 mm, respectively. The substrate temperature (T_{sub}) was not controlled during the deposition process.

In order to obtain crystallographic characteristics, X-ray diffraction (XRD) measurements were performed with a RIGAKU Rotaflex 12 kW with CN2173D6 goniometer. The film thickness was measured by the gravimetric method. The micro-interferometer (Olympus) was used.

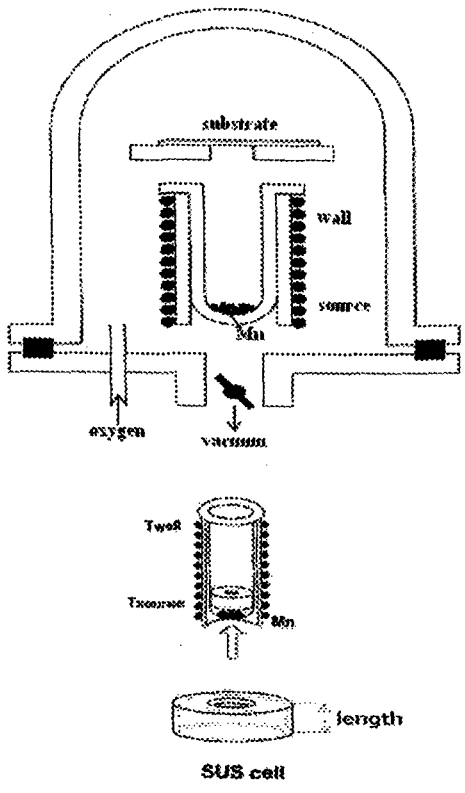

Fig. 1 Schematic of a SUS cell. The stainless steel (SUS) cell with a hole is set in the bottom of the crucible.

3. Results and Discussion

Figure 2 shows the dependence of deposition rate on the deposition run with SUS cells which have different length. The length of SUS cell was varied from 10 to 70 mm. The T_{source} was chosen to get the deposition rate of around 15 Å/s at the first run for each length of SUS cells. This deposition rate was found to be suitable to prepare Mn_3O_4 films.[33] Only the deposition rate of 11.6 and 7.88 Å/s could be obtained for the length of SUS cell of 50 and 70 mm, respectively. It is due to the limitation of heat capacity of source heater.

In the case with a length of 30 mm, the deposition rate does not deteriorate so much for first several deposition runs as compared with others. This SUS cells work very well.

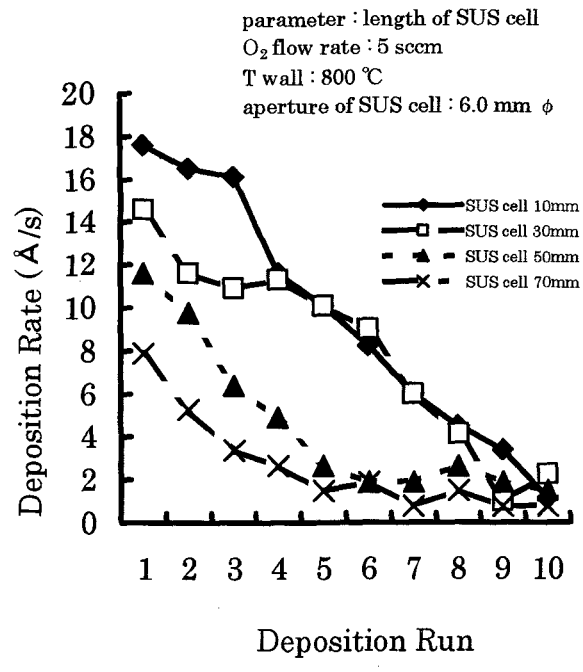

Figures 2 The dependence of deposition rate on the deposition run with SUS cells which have different height. The height of SUS cell was varied from 10 to 70 mm.

Figure 3(a) shows the variation of XRD peak strength of (103) of Mn_3O_4 films with increasing deposition run. The parameter is the length of SUS cell. These films are so called a Hausmannite. These films have (103) and (204) orientations as shown in the early paper. In the case of 10 mm, the deposition rate is slightly high to get this structure until fourth deposition run. Large (103) peaks were obtained in the case of SUS cell length of 30 and 50 mm. It is shown that the deposition rate between 5 to 12 Å/s results in the preparation of (103) oriented films.

a)

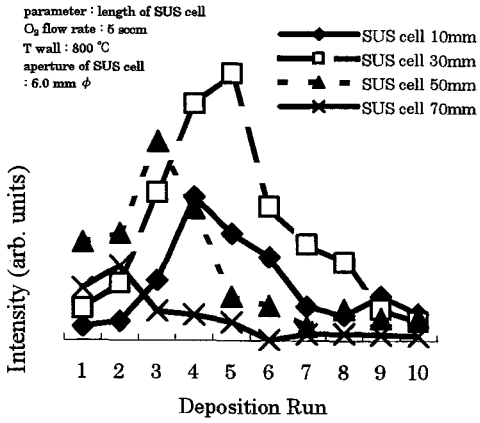

b)

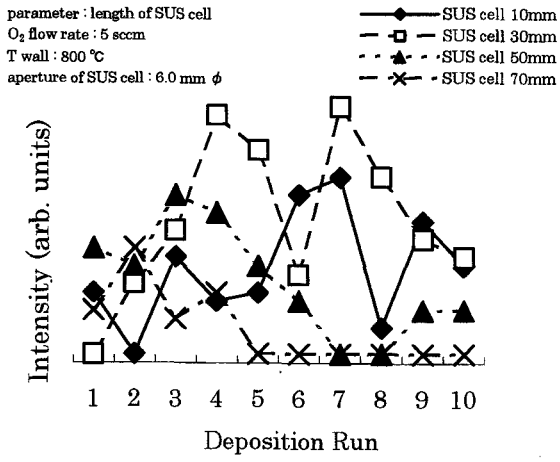

c)

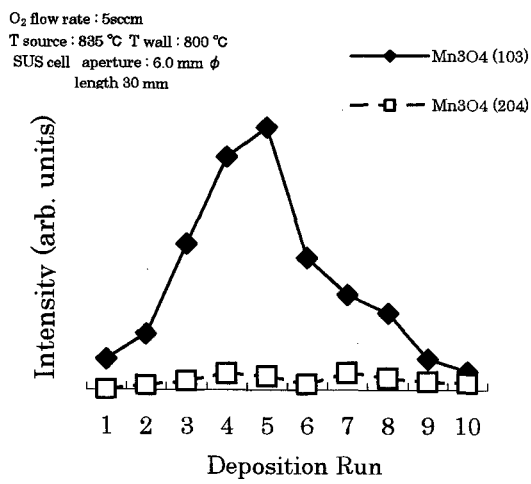

Fig.3 (a) The variation of XRD peak strength of (103) of Mn_3O_4 films with increasing deposition run. (b) The variation of XRD peak strength of (204) of Mn_3O_4 films with increasing deposition run. (c) The variation of XRD peak strength of (103) and (204) of Mn_3O_4 films with increasing deposition run in the case of SUS cell length of 30 mm.

Figure 3(b) shows the variation of XRD peak strength of (204) of Mn_3O_4 films with increasing deposition run. There are no obvious peaks in the case of SUS cell length of 10 and 30 mm. There are small peaks at third and second run in the case of SUS cell length of 50 and 70 mm, respectively.

Figure 3(c) shows the variation of XRD peak strength of (103) and (204) of Mn_3O_4 films with increasing deposition run in the case of SUS cell length of 30 mm. The preferred orientation of (103) can be identified in this figure.

Figure 4 shows the variation of XRD peak strength of (103) of Mn_3O_4 films with increasing deposition run in the case of SUS cell length of 30 mm. The XRD strength is usually decreases with decreasing the film thickness. So, the XRD strength was normalized with the thickness of films. As a result, It is recognized that these films have obvious XRD strength even after the sixth run.

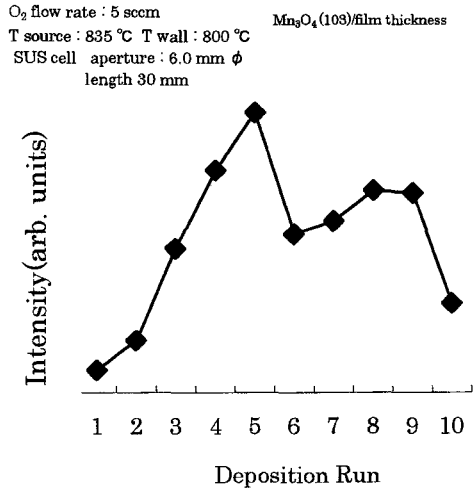

Fig. 4 The dependence of substrate temperature (T_{sub}) on the height of SUS cell.

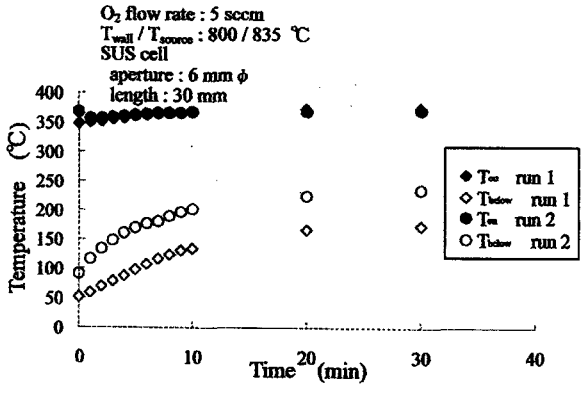

Fig. 5 The dependence of variation of substrate temperature (T_{sub}) on the deposition time . The length of SUS cell is 30 mm.

Figure 5 shows the dependence of variation of substrate temperature (T_{sub}) on the deposition time . The length of SUS cell is 30 mm. The T_{sub} was measured on the back side of substrate and just bellow the substrate. They are called T_{on} and T_{below}. The first and second run is shown here. The temperature of T_{below} is gradually increased as increasing the deposition time. This temperature rise is saturated after 10 minute deposition. The temperature difference between T_{on} and T_{below} is still about 100 ℃ even after saturation.

There are three parameters that govern the composition and crystallinity of films. They are O_2 flow rate, Mn deposition rate, and T_{sub}. O_2 flow rate was fixed at 5 sccm and T_{sub} was not controlled through this study. So the film properties depend on the correlation between O_2 flow rate and Mn deposition rate. A desired composition, for example Mn_3O_4 in this work, could be obtained with a restricted range of deposition rate, for example, between 5 to 12 Å/s. So it is crucial to maintain the deposition rate at this restricted range to prepare Mn_3O_4 films.

The SUS cell successfully protects oxidation of Mn evaporant in the crucible. So the Mn deposition rate could be maintained at appropriate values. The reproducibility of film composition is improved by using the SUS cell. The deposition rate depends on the length of SUS cell. It is found that the optimum length of SUS cell is 30 mm under the condition of T_{wall} and T_{source} of 800 and 835 ℃, respectively. These values are about 100 K lower than those obtained former cases.[31] This is due to quartz caps which cover the thermocouples. These caps could be attached to the crucible surface with the same geometry even after changing SUS cell. It contributes to improve the reproducibility of temperature measurement of T_{wall} and T_{source}.

The Mn_3O_4 structure could be prepared at the deposition rate under 12 Å/s.

One of the problems to be solved is how $LiMn_2O_4$ structure should be prepared from our Mn_3O_4 films. We hope we will report on that aspect later. We are convinced that the idea shown in the present work could be applicable to the preparation of other oxide films.

4. Conclusion

A SUS cell was introduced in the bottom of the Mn crucible, which successfully protected Mn evaporant from being oxidized during the reactive evaporation process. The properties of SUS cell which overcomes the oxidation of Mn metal in the crucible was investigated.

It is found that the optimum length of SUS cell is 30 mm. This SUS cell contributes to the successes of controlling the stoichiometry as well as of protecting the oxidation of Mn evaporant.

The Mn_3O_4 structure could be prepared under the conditions of Mn deposition rate below 12 Å/s and O_2 flow rate of 5 sccm.

This method could improve the reproducibility of Mn oxide films for Li secondary batteries.

Ackowledgments

This work was supported in part by Shizuoka Research Institute and Hamamatsu Science and Technology Promotion Society. Support also from the Grant-in-Aid for Scientific research (C) in the Ministry of Education, Culture, Sports, Science and Technology in Japan.

REFERENCES

1. J. Desilvestro and O. Haas:
J. Electrochem. Soc. **137** (1990) 5C.
2. R. Koksbang, J. Barker, H. Shi and M.Y. Saidi:
Solid State Ionics **84** (1996) 1.
3. M. M. Thackeray, A de Kock, M. H. Rossouw,
D. Liles, R. Bittihn and D. Hoge:
J. Electrochem. Soc. **139** (1992) 363.
4. R. J. Gummow, A. de Kock and M. M. Thackeray:
Solid State Ionics, **69** (1994) 59.
5. J. C. Hunter: J. Solid State. Chem. **39** (1981) 142.
6. M. M. Thackeray, P. J. Johonson, L. A. de Picciotto,
P. G. Bruce and J. B. Goodenough:
Mater. Res. Bull. **19** (1984) 179.
7. M. M. Thackeray, W. I. F. David, P. G. Bruce and
J. B. Goodenough: Mater. Res. Bull. **18** (1983) 461.
8. K. M. Colbow, J. R. Dahn and R. R. Hearing:
J. Power Sources 26(1989)397.
9. M. M. Thackeray:
J. Electrochem. Soc. **142** (1995) 2558.
10. J. Cho and M. M. Thackeray:
J. Electrochem. Soc. **146** (1999) 3577.
11. C. R. Horne, U. Bergman, S. J. Wen, and
E. J. Cairns: J. Electrochem. Soc. **147** (2000) 395.
12. Y. J. Lee, F. Wanf, S. Murerjee, J. McBreen. and
C. P. Grey: J. Electrochem. Soc. **147** (2000) 803.
13. Y. Xia, T. Sakai, C. Wang, T. Fujieda, K. Tatsumi,

K. Takahashi, A. Mori, and M.Yoshio:
J. Electrochem. Soc. **148** (2001) A112.
14. Y. Bando, S. Horii and T. Tanaka:
Jpn. J. Appl. Phys. **17** (1978) 1037.
15. F. K. Shokoohi, J. M. Tarascon, B. J. Wilkens,
D. Guyomard and C. C. Chang: J. Electrochem.
Soc. **139** (1992) 1845.
16. K. A. Striebel, C. Z. Deng, S. J. Wen and
E. J. Cairns: J. Electrochem. Soc. **143** (1996) 1821.
17. A. Rougier, K. A. Striebel, S. J. Wen and
E. J. Cairns: J. Electrochem. Soc. **145** (1998) 2975.
18. P. Liu, J. G. Zhang, J. A. Turner, C.E. Tracy and
D. K. Benson:
J. Electrochem. Soc. **146** (1999) 2001.
19. N. J. Dudney, J. B. Bates, R. A. Zuhr, S. Young,
J. D. Robertson, H. P. Jun and S. A. Hackney:
J. Electrochem. Soc. **146** (1999) 2455.
20. M. Mohamedi, D. Takahashi, T. Itoh, M. Umeda,
and I. Uchida: J. Electrochem. Soc. **149** (2002) A19.
21. K. A. Striebel, E. Sakai, and E. J. Cairns:
J. Electrochem. Soc. **149** (2002) A61.
22. K. Y. Chung and K. B. Kim:
J. Electrochem. Soc. **149** (2002) A79.
23. M. Isai, K. Yamaguchi, H. Iyoda, H. Fujiyasu and
Y. Ito: J. Mater. Res. **14** (1999) 1653.
24. M. Isai, K. Yamaguchi, T. Nakamura, Y. Ito and
H.Fujiyasu: Trans. Mater. Res. Soc. Jpn. **24** (1999) 157.
25. M. Isai, K. Yamaguchi, T. Nakamura, H. Fujiyasu
and Y. Ito: Proc. Symp. Giga Scale Integration
Technology, Washington State University, Pullman,
Washington, 1998, p.165.
26. M. Isai, H. Ichikawa, T. Shimada, H. Fujiyasu and
Y. Ito: Trans. Mater. Res. Soc. Jpn. **25** (2000) 1127.
27. M. Isai, H. Ichikawa, T. Shimada, K. Morimoto,
H. Fujiyasu and Y. Ito:
Jpn. J. Appl. Phys. **39** (2000) 6676.
28. M. Isai, H. Ichikawa, H. Takahashi, H. Fujiyasu and
Y. Ito: Electrochemistry **68** (2000) 963.
29. M. Isai, H. Ichikawa, T. Shimada, K. Morimoto and
H. Fujiyasu:
Trans. Mater. Res. Soc. Jpn. **26** (2001) 1219.
30. M. Isai, H. Fujiyasu and T. Kashiwakura:
Trans. Mater. Res. Soc. Jpn. **27** (2002) 799.
31. M. Isai, T. Shimada, T. Matsui and H. Fujiyasu:
Jpn. J. Appl. Phys. **40** (2001) 5069.
32. M. Isai and H. Fujiyasu:
Jpn. J. Appl. Phys. **40** (2001) 6552.
33. M. Isai, E. Nishida, H. Shimizu, S. Honda and H.
Fujiyasu:
Trans. Mater. Res. Soc. Jpn. **28** (2003) 1311.

(Received December 24, 2004; Accepted February 28, 2005)